UNIVERSITÉ DE GENÈVE

Archive ouverte UNIGE
https://archive-ouverte.unige.ch

Article scientifique | Article | 2022

Published version | Open Access

This is the published version of the publication, made available in accordance with the publisher's policy.

High Environmental Radioactivity in Artisanal and Small-Scale Gold Mining in Eastern Democratic Republic of the Congo

Atibu, Emmanuel K.; Arpagaus, Philippe; Mulaji, Crispin K.; Mpiana, Pius T.; Pote-Wembonyama, John; Loizeau, Jean-Luc; Carvalho, Fernando P.

How to cite

ATIBU, Emmanuel K. et al. High Environmental Radioactivity in Artisanal and Small-Scale Gold Mining in Eastern Democratic Republic of the Congo. In: Minerals, 2022, vol. 12, n° 10, p. 1278. doi: 10.3390/min12101278

This publication URL: https://archive-ouverte.unige.ch/unige:164885
Publication DOI: 10.3390/min12101278

© This document is protected by copyright. Please refer to copyright holder(s) for terms of use.

minerals

MDPI

Article

High Environmental Radioactivity in Artisanal and Small-Scale Gold Mining in Eastern Democratic Republic of the Congo

Emmanuel K. Atibu [1], Philippe Arpagaus [2], Crispin K. Mulaji [1], Pius T. Mpiana [1], John Poté [1,2], Jean-Luc Loizeau [2] and Fernando P. Carvalho [3,*]

[1] Department of Chemistry, Faculty of Science, University of Kinshasa, Kinshasa XI B.P. 190, Democratic Republic of the Congo
[2] Department F.-A. Forel for Environmental and Aquatic Sciences and Institute for Environmental Sciences, University of Geneva, 1211 Geneva 4, Switzerland
[3] Laboratório de Protecção e Segurança Radiológica, Instituto Superior Técnico, Campus Tecnológico Nuclear, Universidade de Lisboa, 2695-066 Lisboa, Portugal
* Correspondence: carvalho@ctn.tecnico.ulisboa.pt

Abstract: The radioactivity associated with artisanal and small-scale gold mining activities (ASM) carried out along the Ulindi River, in the eastern Democratic Republic of the Congo, was evaluated by gamma-ray spectrometry and inductively coupled plasma–mass spectrometry of soil and sediment samples. The results revealed that activity concentrations of ^{238}U (up to 3127 ± 98 Bq kg^{-1}), ^{226}Ra (up to 2710 ± 89 Bq kg^{-1}) and ^{232}Th (up to 2142 ± 162 Bq kg^{-1}) were 71- to 89-fold higher than the worldwide average concentrations reported by UNSCEAR in soils. Primordial radionuclides are, thus, present in high concentrations in deposits of gold in that region and the average ambient effective radiation dose rate was determined at 8.4 mSv y^{-1} (range 0.5 to 40 mSv y^{-1}). This area may be classified as a natural high background radiation area (HBRA). The radiation risk for artisanal miners and population members manipulating those geological materials were assessed through radiological parameters. such as the radium equivalent activity index (Ra_{Eq}), outdoor gamma absorbed dose rate (ODRA), annual effective dose equivalent (AEDE), and excess lifetime cancer risk (ELCR). The mean values of these parameters were significantly elevated in comparison to the world average levels and indicated the existence of significant radiation risks for gold miners and members of the local population. A radiation safety policy seems needed to protect workers and the local population in this region.

Keywords: artisanal small-scale gold mining; naturally occurring radionuclides; gamma-ray spectrometry; inductively coupled plasma–mass spectrometry; risk assessment

check for updates

Citation: Atibu, E.K.; Arpagaus, P.; Mulaji, C.K.; Mpiana, P.T.; Poté, J.; Loizeau, J.-L.; Carvalho, F.P. High Environmental Radioactivity in Artisanal and Small-Scale Gold Mining in Eastern Democratic Republic of the Congo. *Minerals* **2022**, *12*, 1278. https://doi.org/10.3390/min12101278

Academic Editor: Tsutomu Sato

Received: 26 August 2022
Accepted: 5 October 2022
Published: 11 October 2022

Publisher's Note: MDPI stays neutral with regard to jurisdictional claims in published maps and institutional affiliations.

Copyright: © 2022 by the authors. Licensee MDPI, Basel, Switzerland. This article is an open access article distributed under the terms and conditions of the Creative Commons Attribution (CC BY) license (https://creativecommons.org/licenses/by/4.0/).

1. Introduction

The Democratic Republic of the Congo (DR Congo or DRC) has a vast wealth of mineral resources, including gold, wolfram, nickel, copper, cobalt, and uranium, of which the extent has not been fully evaluated yet [1,2]. In the eastern part of DRC, in particular in the Ulindi River basin in Maniema and South Kivu provinces, the artisanal and small-scale mining (ASM) activities have been ongoing for many years with the production of large amounts of gold, cassiterite (tin mineral), wolfram, niobium, and columbite-tantalite (coltan) [3].

The current production of metals and minerals from DR Congo contributes to a large fraction of the world production. For example, in 2018, the DR Congo was the world first cobalt producer accounting for approximately 71% (111,713 tons) of the global production, while it was the 1st world producer of tantalite, the 3rd producer of industrial diamonds, the 4th world producer of niobium and copper, and the 7th producer of tin [3].

Despite this large mineral production, the country has not been able to distribute revenues and to improve living conditions for the majority of the DRC population (approxi-

mately 95 million inhabitants). In this context, the artisanal and small-scale mining became a way of survival for 250,000 informal miners and their families eastern DR Congo, despite the unsafe conditions in which this work was carried out [4]. Although these artisanal mining activities are illegal, their ban could have even higher social costs. Indeed, several international non-governmental organizations (NGOs) have recommended that artisanal mining should be allowed, albeit with improved safety, and the mining production purchased by the state was a way to enhance revenue distribution [5,6]. One way or another, artisanal and small-scale mining will continue for long time and the improvement of health and safety conditions must be pursued.

Metal deposits in the copper belt region, encompassing DR Congo, Zambia, and Angola, often display the co-occurrence of uranium [7]. Several reports referred to uranium occurrence in high concentrations in metal production, such as copper and coltan [7–9]. A recent environmental study in DR Congo reported enhanced concentrations of radionuclides from the uranium and thorium radioactive decay series associated with copper and cobalt artisanal mining at the Luilu and Dilala rivers [10].

In the past, there was exploitation of uranium in the Katanga province, especially at the Shinkolobwe mine, which was exported mainly to the USA for the Manhattan Project [11]. Uranium resources in that area are significant and more recently, a new concession was awarded for uranium exploitation, but production has not yet resumed.

In the regions with ASM activities, few studies have been made about the environmental concentrations of uranium and other natural radionuclides and on the human exposure to toxic metals and radioactive elements. Nevertheless, two of them have reported high uranium concentrations in the urine of artisanal miners and members of the population, including children living nearby [8,12]. One of these studies also concluded that the levels of accumulated cobalt were the highest measured in humans worldwide. Furthermore, the enhanced levels of uranium in the urine of miners from Kolwezi town (Katanga Province), in comparison to a reference population group, provided evidence for the bioavailability of natural uranium to humans and, hence, the potential occurrence of toxic effects [8,12].

In the years 2013–2014, a gold rush occurred near the town of Shabunda, targeting alluvial gold deposits in the Ulindi River. This gold rush conduced to a large increase in the number of dredges, dedicated to exploiting the alluvial gold deposits in the Ulindi riverbed and in the riverbanks. In those years, the number of manually operated dredges in the Ulindi River rose to 150, plus 4 semi-industrial mechanized dredges. The number of artisanal miners in the region was not accurately recorded but it was roughly estimated at "tens or even hundreds of thousands of South Kivutians" [5]. Furthermore, many more population members are involved in logistic operations related to the artisanal and small-scale mining.

In the Ulindi River, the manual dredges use divers that work in the turbid water to guide an aspiration hose that delivers the sediment slurry on the dredge, where it is wet sieved to retrieve gold nuggets and, eventually, other mineral particles. When sediment sieving is carried out on board dredges, the sieved sediment is discharged into the river. However, in some instances, this work is carried out on land and the sieved sediment is stockpiled on the riverbank. The population reuses the materials from such mining waste stockpiles as a construction material for house building.

Following the gold rush in the Ulindi River, in March 2015 the DRC government took action and suspended dredging along the river due to high level of radioactivity detected in sediments, but no detailed report was issued. Despite the governmental ban, illegal mining has been ongoing, in part because of the remoteness of the region [13]. Therefore, there is a continued potential exposure of artisanal miners and local populations to the ionizing radiation from geological materials in this region.

The exposure to ionizing radiation from radioactive materials may be harmful to human health [14,15]. The current international radiation safety standards set dose limits at 20 mSv y^{-1} for radiation workers and at 1 mSv y^{-1} for members of the public for the radiation doses originated from duly licensed practices involving the application of radiation and/or

handling of radioactive materials [15]. In the DRC, the assessment of radiation exposures from naturally occurring radionuclides and from human activities is mostly to be made yet. In the case of such ASM activities, according to current international safety standards and DRC nuclear regulations, the radiation dose limit applicable is 1 mSv y^{-1}.

This study provides the first data for eastern DR Congo and focus on the Ulindi River region, where artisanal and small-scale gold mining activities are carried out. The aims of this study were: (1) to identify and determine the concentrations of naturally occurring radionuclides in soils and sediments from the Ulindi River basin; (2) to assess the radiological hazards in order to evaluate the health risks to miners and to the local population.

2. Materials and Methods

2.1. Description of the Study Area and Sample Collection

This study was conducted in Maniema Province, located to the east of the Democratic Republic of the Congo in Central Africa (Figure 1A,B). This province has a significant mining potential, including a large artisanal exploitation of tin ore (cassiterite) and associated elements, such as tungsten (wolframite), niobium, columbium-tantalum (coltan), and gold.

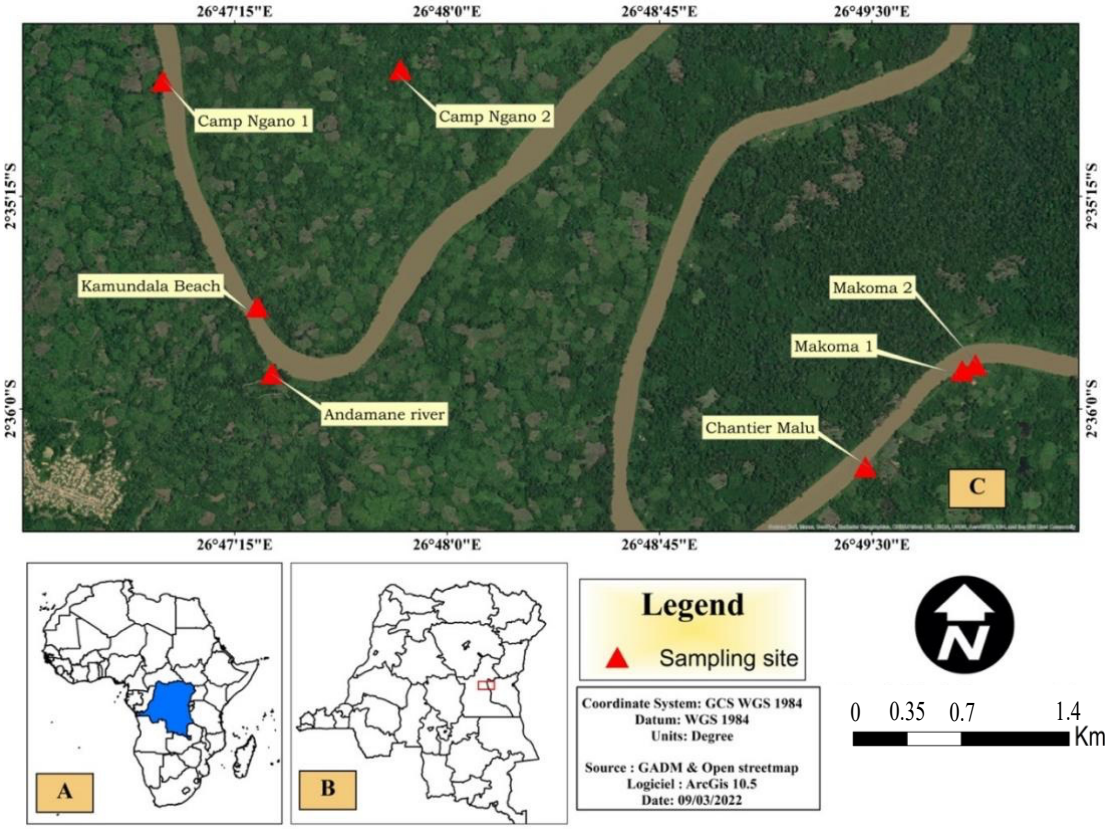

Figure 1. Study area. (**A**) DRC in Africa, (**B**) sampling site (red rectangle) in Maniema Province (DRC), (**C**) Sediment and/or soil sampling sites along Ulindi River and one of its tributaries (Camp Ngano 2).

The geology of Maniema province comprises a granite formation, in particular in the Kalima region, and schists. The soils were formed from erosion and disaggregation of granites and quartz veins. Over time, the rivers flowing through this province contributed to the formation of a thick red soil and alluvial deposits containing gold and other metals [1,16,17].

The vegetation cover is rainforest in the north of the Maniema province and savannah in the south, maintained by abundant precipitations (1200–2000 mm annual rainfall). The province of Maniema has a population of approximately 1.8 million inhabitants.

The source of the Ulindi River is located in the South Kivu province of DRC. The river flows through the Pangi and Kailo territories to reach the town of Kowe in Punia territory. The Ulindi River is known for its important ASM activity, which is focused on the exploitation of gold-rich alluvial sediment deposits. This artisanal and small-scale exploitation uses mercury to form the amalgam with gold, which is also a major environmental and public health concern [18].

The gold exploitation in the Ulindi River has been formally suspended in 2015 because of the high levels of radioactivity detected in riverbed sediments and fear that illegal uranium extraction and uncontrolled sales could take place. Nevertheless, the artisanal gold mining is actively continuing and metal production is drained through traders to the international markets, as before [19].

Other than the fluvial mining, riverine populations make intensive use of the Ulindi River as a source for drinking water, bathing, and irrigation of agricultural plots for vegetable production (Figure 2). Earthen houses are built with clayey materials from the riverbed and soils.

Figure 2. Artisanal and small-scale mining activities and miner's settlements along the Ulindi River. (**a**): dredge used for gold mining, (**b**): addition of Hg to form the amalgam with gold, (**c**): miner dwellings, (**d**): food cooking on the river bank (Photos by E. Atibu).

Soil and sediment samples were collected in the upper reach of Ulindi River from 10 to 11 March 2018 (Figure 1C). Sample labels, GPS coordinates, and human activities carried out by the sampling sites are reported in Table 1. Sediment samples collected (n = 7) were labelled Se1, Se2, Se3, Se4, Se5, Se6, and Se7. Soil samples collected (n = 6) were labelled So1, So3, So4, So5, So6, and So7.

Table 1. GPS location and description of sampling sites.

Sampling Site	Sample Label	Human Activities	Latitude Longitude
Camp Ngano 1	So1 Se1	Former semi-industrial gold processing unit. Bathing, laundry of clothes, river water consumed as drinking water. Fields of cassava, maize, banana, and rice irrigated with river water.	S 02°34′50.6″ E 026°46′59.8″
Camp Ngano 2	- Se2	Former semi-industrial gold processing unit. Bathing, laundry of clothes, river water consumed as drinking water. Fields of cassava, maize, banana, and rice irrigated with river water.	S 02°34′48.2″ E 026°47′50.1″
Andamane river	So3 Se3	Point where the tributary Andamane River joins the Ulindi River. Former semi-industrial gold processing unit. Bathing, laundry of clothes, river water consumed as drinking water. Fields of cassava irrigated with river water.	S 02°35′52.5″ E 026°47′22.9″
Kamundala Beach	So4 Se4	Right bank of Kamundala Beach. Former semi-industrial gold processing unit. Bathing, laundry of clothes, water consumed as drinking water.	S 02°35′38.4″ E 026°47′19.8″
Chantier Malu	So5 Se5	Former semi-industrial gold processing unit. Bathing, laundry of clothes, river water consumed as drinking water.	S 02°36′12.4″ E 026°49′28.6″
Makoma 1	So6 Se6	Gold Processing Unit (Activity ongoing). Bathing, laundry of clothes, river water consumed as drinking water.	S 02°35′51.9″ E 026°49′49.1″
Makoma 2	So7 Se7	Former semi-industrial gold processing unit. Bathing, laundry of clothes, river water consumed as drinking water.	S 02°35′50.8″ E 026°49′51.9″

So, Se: soil and sediment, respectively.

At each sampling point in the Ulindi River, at a distance of about 1 m from the shore and at 0–20 cm water depth, approximately 250–300 g of surface sediment was collected from the river bed with a plastic shovel, in triplicate, and pooled in one larger composite sample. Soil samples were collected on the river banks, in areas of former mining operations (sieving and ore washing) and agriculture areas, according to the strategy used in our previous studies [10,20,21]. After collection, all samples were transferred into 1.5 L clean plastic bottles and transported for analysis in the laboratories of the University of Geneva, Switzerland.

2.2. Sample Treatment

Soil and sediment samples were preserved frozen until the treatment for analyses, which included freeze-drying, material disaggregation, sieving through a 2 mm stainless steel screen to remove gravel, stones, pebbles and other occasional macro-impurities in order to obtain a homogeneous material for analysis [22]. The grain-size fraction less than 2 mm, which made the largest fraction of the sample collected, contains most of radioactivity. The removal of macro impurities and standardization of the grain size sieving cut off aimed to enhance comparability between samples. The <2 mm fraction of sample materials was then crushed with a grinder (Fritsch, Germany) and homogenized. Weighted aliquots of homogenized samples were used for radionuclide analysis [10].

2.3. Radionuclide Analysis by Gamma-ray Spectrometry

The <2 mm sample aliquots were compacted in glass tubes leaving no headspace. The tubes were hermetically sealed with paraffin wax and cellophane tape and kept aside for about one month to ensure the formation of secular radioactive equilibrium between radium (^{226}Ra), radon gas (^{222}Rn), and radon short-lived decay products (^{214}Pb, ^{214}Bi,) before gamma-ray spectrometric analysis.

The gamma-ray spectrometry was the instrumental technique used for the determination of activity concentrations of radionuclides (^{238}U, ^{226}Ra, ^{210}Pb, ^{40}K) in the samples, applying long acquisition times (several days). The activity concentrations of ^{238}U was

determined using the most intensive gamma-transitions energy of 63.29 keV and 92.59 keV from its first progeny, ^{234}Th. For determination of ^{226}Ra, the gamma energies 295.2 and 351.9 from ^{214}Pb were used. The photopeak at 1460.82 keV was used to determine ^{40}K and the photopeak at 46.5 kev to determine ^{210}Pb.

A high-purity germanium well detector (Model GWL-120230, Ortec, AMETEK GmbH, Meersbusch, Germany), with an active volume of 136 cm^3 and an aluminum window was used for the gamma spectrometry measurements. The detector is shielded from the environmental radioactive background by a 10 cm lead shield with copper and PVC lining. Standard nuclear electronics was used and the software Gamma Vision v.6 (Ortec) was employed for the data acquisition and spectral analysis. The detection efficiencies were determined using multi-gamma radioactive standards (DL-1a Uranium-Thorium reference ore, CANMET, CCRMP, Ontario, Ottawa, Canada), with an energy range from 46.5 to 1460 keV in geometries similar to sample geometries. The detection efficiency of the radioisotopes was corrected for geometry, density, and chemical composition using Monte Carlo simulation software (Gespecor 4.1, [23]), CID-media, Freigericht, Germany.

2.4. Titanium and Thorium Analysis by ICP-MS

About 1 g of each prepared sample (lyophilized, homogenized, and sieved through a 2 mm stainless steel screen) was mixed with 10 mL HNO_3 2M in Teflon bombs, heated during 16h at 105 °C, and centrifuged at 4000 rpm during 15 min at 20 °C. The supernatant was diluted 200 times with 1% HNO_3 (Suprapur®, Merck KGaA, Darmstadt, Germany) solution. Ten mL of diluted solution were used for titanium element analysis by inductively coupled plasma–mass spectrometry (ICP-MS, Agilent 7700x series, Santa Clara, CA, USA). The certified reference materials LKSD-4 and STSD-2 were used for sediment and soil analysis, respectively, to verify the digestion procedure, the instrument sensibility, and the reliability of the results. All measurements were conducted in triplicate. Standard deviations of three replicate measurements were below 5%. The results are expressed in mg kg^{-1} dry soil/sediment weight [24,25].

2.5. Evaluation of Radiological Hazard and Health Effects

The following radiological hazard indices were calculated to assess the radiation risks for human population from exposure to radionuclides contained in soils and sediments, as described in previous studies [10,26].

a. Radium equivalent activity index (Ra_{Eq})

The Ra_{Eq} is a single parameter which is used to describe the gamma output and the radiation hazards associated with the mixture of ^{238}U, ^{232}Th, and ^{40}K in samples. The Ra_{Eq} was calculated using the following equation [27,28]:

$$Ra_{Eq}\ (Bq\ kg^{-1}) = A_U + 1.43\ A_{Th} + 0.077\ A_K \quad (1)$$

where A_U, A_{Th}, and A_K are the activity concentrations in soils and sediments (Bq kg^{-1}) of ^{238}U, ^{232}Th, and ^{40}K, respectively. The equation above indicates that 370 Bq kg^{-1} of ^{238}U, 259 Bq kg^{-1} of ^{232}Th and 4810 Bq kg^{-1} of ^{40}K produce the same gamma ray dose rate [28]. The Ra_{Eq} world average is 370 Bq kg^{-1} [28].

b. Outdoor gamma absorbed dose rate (ODRA)

The biological and clinical effects of ionizing radiation are directly linked to the absorbed dose rate [29,30]. The outdoor gamma absorbed dose rate (ODRA) at 1 m above the ground surface, originated by the gamma radiation emitted by ^{238}U, ^{232}Th, and ^{40}K radionuclides, assumed to be uniformly distributed in the soil, was calculated according to UNSCEAR [28]. The factors used to convert activity concentrations of ^{238}U, ^{232}Th, and ^{40}K into the dose rate were 0.462 nGy h^{-1}, 0.604 nGy h^{-1} and 0.042 nGy h^{-1}, respectively, for those radionuclides.

Therefore, ODRA was calculated as follows:

$$\text{ODRA (nGy h}^{-1}) = 0.462A_U + 0.604\ A_{Th} + 0.042A_K \quad (2)$$

where A_U, $A_{Th,}$ and A_K are the activity concentrations in Bq kg^{-1} of ^{238}U, ^{232}Th, and ^{40}K, respectively. The world average of ODRA from soils is 59 nGy h^{-1} [28,31].

c. Annual effective dose equivalent (AEDE)

The annual effective dose equivalent (AEDE) received by a member of the public was calculated using the following equation:

$$\text{AEDE} = \text{ODRA} \times \text{DCF} \times \text{OF} \times \text{T} \quad (3)$$

where DCF is the dose conversion factor (0.7 Sv Gy^{-1}). The DCF is used to convert the outdoor gamma absorbed dose rate to the human effective dose, for an outdoor occupancy factor (OF) of 20% [32]. T is the exposure time (8760 h y^{-1}) [28]. The AEDE was calculated using the following equation:

$$\text{AEDE (mSv y}^{-1}) = \text{ODRA (nGy h}^{-1}) \times 0.7\ \text{Sv Gy}^{-1} \times 0.2 \times 8760\ \text{h y}^{-1} \times 10^{-6} \quad (4)$$

The world average value of AEDE is 0.07 mSv y^{-1} [28,31].

d. Excess lifetime cancer risk (ELCR)

The excess lifetime cancer risk (ELCR) parameter enables the estimation of the probability of cancer incidence in a human population for a specified lifetime from exposure to naturally occurring radionuclides. The ELCR was calculated using the equation:

$$\text{ELCR} = \text{AEDE} \times \text{DL} \times \text{RF} \quad (5)$$

where DL is the duration of life (assumed as 70 years), and RF is the risk factor of contracting a fatal cancer per Sievert (Sv^{-1}) received. For stochastic effects, the ICRP 60 recommends the RF value of 0.05 for the members of the public [33,34]. The world average value of ELCR is 0.00029 [28,31].

e. Hazard indices

To make an internal and external assessment of the health effects from radioactivity of earth's surface materials containing ^{238}U, ^{232}Th, and ^{40}K and used as construction materials, Beretka and Mathew [35] defined two indices, in which the objective is to limit the radiation dose received to 1mSv y^{-1} [33].

The external hazard index (H_{ex}) is defined as:

$$H_{ex} = ((A_U/370\ \text{Bq kg}^{-1}) + (A_{Th}/259\ \text{Bq kg}^{-1}) + (A_K/4810\ \text{Bq kg}^{-1})) \leq 1 \quad (6)$$

where A_U, A_{Th}, and A_K are the activity concentration in Bq kg^{-1} of ^{238}U, ^{232}Th and ^{40}K, respectively [36]. The radiation hazard is considered acceptable when H_{ex} does not exceed the unity.

The internal hazard index (H_{in}) gives information on the internal exposure to carcinogenic radon and its short-lived products, which are hazardous through inhalation [37]. H_{in} was calculated through the equation:

$$H_{in} = ((A_{Ra}/185\ \text{Bq kg}^{-1}) + (A_{Th}/259\ \text{Bq kg}^{-1}) + (A_K/4810\ \text{Bq kg}^{-1})) \leq 1 \quad (7)$$

where A_{Ra}, A_{Th} and A_K are the activity concentrations (in Bq kg^{-1}) of ^{226}Ra, ^{232}Th and ^{40}K, respectively [27,38]. H_{in} value must not exceed the unity for the radiation hazard to be considered negligible.

2.6. Statistical Analysis

Triplicate measurements were carried out on the analyzed samples and averaged. The statistical data treatment (Spearman's rank-order correlation) was performed using the Addinsoft product XLSTAT (Suite, NY, USA [39]) in order to understand the possible positive or negative relationship between analyzed and calculated parameters and their potential sources.

3. Results and Discussion

3.1. Activity Concentrations of Radionuclides in Sediment and Soil Samples

The activity concentrations of natural occurring radionuclides (^{238}U, ^{226}Ra, ^{210}Pb, ^{232}Th and ^{40}K) in soil and river sediment samples are shown in Table 2. All samples displayed much higher activity concentrations of ^{238}U, ^{226}Ra, and ^{232}Th, in comparison with the worldwide average activity concentrations in soils [28]. Furthermore, in general, and also in average, the sediment samples from Ulindi River showed, in a consistent manner, much higher radioactivity values than soil samples from the region, particularly for ^{238}U and ^{232}Th radionuclides and their progenies. This was not verified with ^{40}K, which was more abundant in soils than in sediments.

Table 2. Activity concentrations (Bq kg^{-1} ± 1 SD dry weight) of naturally occurring radionuclides in soil and sediment samples from the Ulindi River basin. Numbers in bold indicate values above the worldwide average concentrations.

Sampling Site	Sample Label	^{238}U	^{226}Ra	^{210}Pb	^{232}Th (*)	^{40}K
Camp Ngano 1	So1	**77 ± 3**	**76 ± 3**	70 ± 3	**80 ± 1**	293 ± 10
Andamane river	So3	**43 ± 2**	**92 ± 4**	79 ± 3	**106 ± 6**	299 ± 10
Kamundala Beach	So4	**60 ± 2**	-	110 ± 6	**42 ± 0.2**	**418 ± 16**
Chantier Malu	So5	**105 ± 4**	-	118 ± 7	**120 ± 7**	**412 ± 16**
Makoma 1	So6	**117 ± 4**	**222 ± 10**	157 ± 7	**274 ± 4**	**414 ± 21**
Makoma 2	So7	**130 ± 5**	**115 ± 6**	137 ± 7	**115 ± 3**	397 ± 16
Average ± SD		**89 ± 10**	**126 ± 27**	112 ± 6	**123 ± 4**	372 ± 15
Camp Ngano 1	Se1	**376 ± 12**	**635 ± 22**	246 ± 10	**1381 ± 22**	131 ± 8
Camp Ngano 2	Se2	**1500 ± 47**	**2710 ± 89**	256 ± 15	-	**440 ± 26**
Andamane river	Se3	**74 ± 3**	**65 ± 3**	54 ± 2	**429 ± 5**	185 ± 7
Kamundala Beach	Se4	**131 ± 4**	**241 ± 9**	125 ± 5	**469 ± 6**	199 ± 9
Chantier Malu	Se5	**1449 ± 46**	**2600 ± 83**	467 ± 18	**2011 ± 64**	42 ± 13
Makoma 1	Se6	**3127 ± 98**	**2020 ± 64**	142 ± 9	**2142 ± 43**	**447 ± 18**
Makoma 2	Se7	**225 ± 7**	**422 ± 15**	146 ± 6	**619 ± 10**	242 ± 12
Average ± SD		**983 ± 31**	**1242 ± 41**	205 ± 9	**1175 ± 25**	241 ± 13
Worldwide average in soils (UNSCEAR, 2000)		35	35		30	400

(*) Calculated based on the concentrations (mg kg^{-1}) of ^{232}Th in samples, considering that ^{232}Th isotope accounts for practically 100% of elemental thorium mass and that the specific activity of natural thorium is 4.06 kBq g^{-1}. In bold, activity concentrations of the radionuclide's higher than the worldwide average in soils (CCME, 1999).

It was observed that ^{238}U, the parent radionuclide of uranium decay series, was better preserved in soils, where it was only in slight deficiency, compared to the concentrations of its radioactive descendants ^{226}Ra and ^{210}Pb. In contrast with this, the sediment samples showed a different geochemical behavior. The ^{238}U had been partly dissolved leaving ^{226}Ra in higher concentrations in sediments, but with the radon gas emanation from sediments, a disruption of the radioactive chain did occur and much smaller amounts of ^{210}Pb remained in the sediments.

The difference in activity concentrations between soils and sediments indicated that the sediment deposits from the riverbed contained the heaviest mineral fractions (particles with denser minerals), while the alluvial deposits of red soils at the river banks were formed by accumulation of clays with less dense minerals. This suggests that, over time, the hydraulic transport and mineral sorting made by river water has produced a segregation of mineral

particles, and the alluvial gold deposits (placers) in the riverbed were also the deposition sites of the dense radioactive minerals of uranium and thorium.

This interpretation is underscored by the highest activity concentration values recorded in this study. These were 3127 ± 98 Bq kg^{-1} for ^{238}U, 2710 ± 89 Bq kg^{-1} for ^{226}Ra, 256 ± 15 Bq kg^{-1} for ^{210}Pb, 2142 ± 43 Bq kg^{-1} for ^{232}Th, and 447 ± 18 Bq kg^{-1} for ^{40}K, which correspond to sediments samples collected from Camp Ngano 2 for ^{226}Ra and ^{210}Pb, and from Makoma 1 for the other radionuclides. It must be noted that the Makoma 1 site was the only sampling site where artisanal gold mining activities were ongoing when samples were collected. The same trend was observed in soil samples., i.e., the soil from Makoma 1 site displayed the higher values for almost all radionuclides, except for ^{238}U and ^{40}K. At this sampling point, the artisanal miners are used to bring dredged river sediment for processing (sieving) at the riverbank, originating an enhancement of radioactivity and soil contamination at the site.

Soils and sediments from the Andamane River (So3, Se3) and Kamundala Beach (So4, Se4) displayed activity concentrations of radionuclides closer to world averages (i.e., normal radioactive background), while all other sampling stations displayed naturally occurring radionuclides in elevated concentrations (or "abnormally" high radioactive background).

Figure 3 shows the variation of activity concentrations according to the sampling sites for both soil and sediment samples. The sediment samples from Makoma 1, Chantier Malu, and Makoma 2 contained the highest activity concentrations of radionuclides. For the soil samples, all sites displayed low activity concentrations, under 1000 Bq kg^{-1}, although in some cases there were enhanced concentrations caused by the dispersal of riverbed sediment as mining residues. The value of 1000 Bq kg^{-1} is used by the International Atomic Energy Agency (IAEA) as a threshold to differentiate materials with acceptable natural radioactivity levels from the radioactive materials that may be of concern and must be regulated under the scope of radiation protection authorities [15].

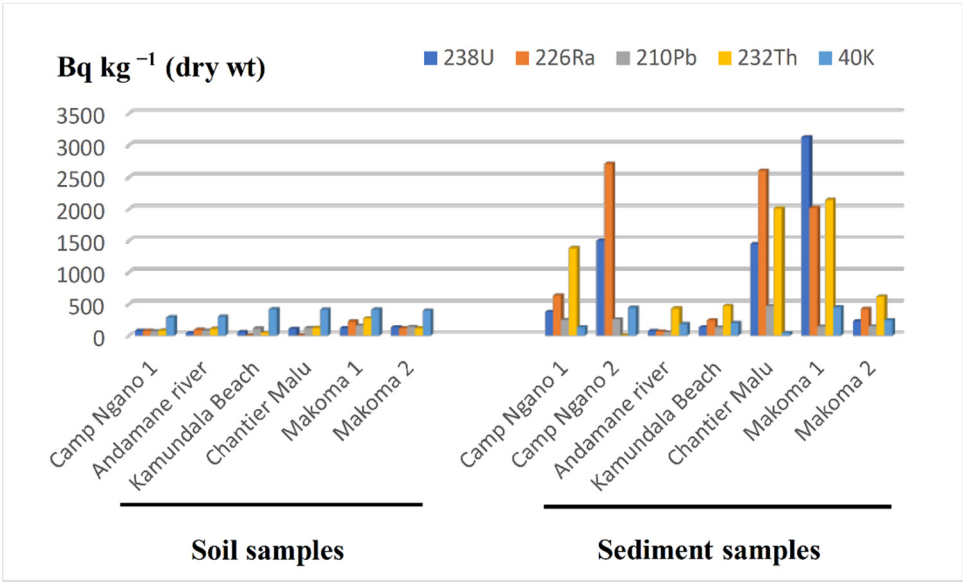

Figure 3. Variation of activity concentration of radionuclides (Bq kg^{-1}) with sampling sites.

The activity concentrations of ^{238}U, ^{232}Th, ^{226}Ra, and ^{40}K determined in the current study were compared to results from our previous study in the copper belt region of the DRC and with other results from the literature (Table 3). The average activity concentrations determined in the Ulindi River basin were higher than values reported from other regions and were similar to concentrations typically found only in uranium-rich areas and in uranium milling waste [40–42]. Based on these results, this region can be considered a natural high background radiation area (HBRA). This issue will be further discussed in the next section.

Table 3. Comparison of the average activity concentrations (Bq kg^{-1}) of ^{238}U, ^{232}Th, ^{226}Ra, and ^{40}K from Ulindi River region with reported concentrations from other regions and from other countries.

Location	^{238}U	^{232}Th	^{226}Ra	^{40}K	References
Congo (DRC) Ulindi River	3127 ± 98	2142 ± 43	2710 ± 89	447 ± 18	This study
Congo (DRC) Luilu River	154 ± 6	28 ± 2	172 ± 14	211 ± 76	[10]
Congo (DRC) Dilala River	378 ± 13	30 ± 6	202 ± 27	95 ± 13	[10]
Tanzania (gold-mining region)	-	-	20.53 ± 0.6	499.89 ± 2.2	[43]
Spain (uranium-mining region)	-	63	2939	-	[44]
Nigeria (gold-mining region)	60.40 ± 4.6	30.80 ± 3.1	-	600.10 ± 3.4	[45]
South Africa (gold-mining region)	2668.90 ± 46.2	67.10 ± 1.4	116	781.00 ± 23.9	[46]
Ghana (gold-mining region)	97.00 ± 2.4	116.70 ± 3.0	-	1795.90 ± 17.8	[47]
Kenya (gold-mining region)	81 ± 3.63	118 ± 8.25	-	260 ± 14.29	[48]
Portugal (uranium-mining region)	1624 ± 48	44.8 ± 18.9	19,966 ± 3353	-	[49]

3.2. Radiological Hazards and Evaluation of Health Effect Indices

Table 4 shows the radiological hazard and health effect indices calculated for all sampling sites. In these calculations, the parameter values for all soil and sediment samples were used and averaged because soils are always present in inhabitant's daily life, and mining workers manipulate the river sediments and are in close contact with sediments while the members of the population use materials from mining waste piles in house construction. Therefore, the exposure to natural occurring radionuclides in geological materials (soils and sediments) from the region is interlinked.

The Ra_{Eq} values varied from 152 Bq kg^{-1} (Kamundala Beach/So4) to 6224 Bq kg^{-1} (Makoma 1/Se6). It must be noticed that the Ra_{Eq} values at So6 (Makoma 1), Se1 (Camp Ngano 1), Se2 (Camp Ngano 2), Se3 (Andamane River), Se4 (Kamundala beach), Se5 (Chantier Malu), Se6 (Makoma 1), and Se7 (Makoma 2) sampling sites were well above the world average level of 370 Bq kg^{-1}.

The ODRA values obtained for the dose at 1 m above the ground ranged between 71 nGy h^{-1} (Kamundala Beach/So4) and 2757 nGy h^{-1}(Makoma 1/Se6) with an average value of 638 nGy h^{-1}, which is 10 times higher than the world average value of 59 nGy h^{-1}.

The AEDE values varied from 0.1 mSv y^{-1} (Andamane River and other sites) to 3.4 mSv y^{-1} (Makoma 1/Se6). The average value (1.0 mSv y^{-1}) of the calculated AEDE was 14 times higher than the world average of 0.07 mSv y^{-1}.

The cancer risk parameter (ELCR) values ranged from 0.3 (Kamundala/So4) to 11.8 (Makoma 1/Se6), with an average value for all sampling sites of 3.0, which was four orders of magnitude higher than the world mean value of 0.00029.

The hazard index H_{ex} and H_{in} values ranged from 0.4 (Kamundala Beach/So4) to 16.8 (Makoma 1/Se6) and from 0.2 (Kamundala Beach/So4) to 21.8 (Chantier Malu/Se5), respectively. The average values of H_{ex} (4.0) and H_{in} (6.0) are both much higher than the recommended maximum value of 1. Sediments and soil materials from the area of Kamundala Beach can be used as construction material, but materials from the remaining areas are not suitable for use as construction materials.

Table 4. Radium equivalent activity index (Ra_{Eq}), outdoor gamma absorbed dose rate (ODRA), annual effective dose equivalent (AEDE), excess lifetime cancer risk (ELCR), and hazard indices (H_{ex} and H_{in}) for the investigated samples.

Sampling Site	Sample Label	Ra_{Eq} (Bq kg^{-1})	ODRA (nGy h^{-1})	AEDE (mSv y^{-1})	ELCR (Unitless)	H_{ex} (Unitless)	H_{in} (Unitless)
Camp Ngano 1	So1	214	96	0.1	0.4	0.6	0.7
Andamane River	So3	218	96	0.1	0.4	0.6	0.9
Kamundala Beach	So4	152	71	0.1	0.3	0.4	0.2
Chantier Malu	So5	308	138	0.2	0.6	0.8	0.5
Makoma 1	So6	541	237	0.3	1.0	1.5	2.3
Makoma 2	So7	325	146	0.2	0.6	0.9	1.1
Camp Ngano 1	Se1	2361	1013	1.2	4.3	6.4	8.8
Camp Ngano 2	Se2	1534	711	0.9	3.1	4.1	14.6
Andamane River	Se3	702	301	0.4	1.3	1.9	2.0
Kamundala Beach	Se4	817	352	0.4	1.5	2.2	3.1
Chantier Malu	Se5	4328	1886	2.3	8.1	11.7	21.8
Makoma 1	Se6	6224	2757	3.4	11.8	16.8	19.2
Makoma 2	Se7	1129	488	0.6	2.1	3.0	4.7
Average		1450	638	1	3	4	6
Minimum		152	71	0.1	0.3	0.4	0.2
Maximum		6224	2757	3.4	11.8	16.8	21.8
Reference value [a]		370	59	0.07	0.00029	≤ 1	≤ 1

[a] [27].

It must be noted that the highest values of Ra_{Eq}, ODRA, AEDE, ELCR, and H_{ex} correspond consistently to the sampling sites Makoma/Se6, where artisanal small-scale gold mining activities was in progress at the time of sampling, except for the H_{in} whose highest value was found in Chantier Malu site (Table 1). Other sites, such as Makoma 1/So6, Camp Ngano 1/Se1, Camp Ngano 2/Se3, Andamane River/Se3, Kamundala beach/Se4, Chantier Malu/Se5, Makoma 1/Se6 and Makoma 2/Se7, were also consistently high for all hazard parameters, in comparison to world averages and to recommended parameter values. Furthermore, in comparison with results for other DRC regions, it appears that the radiological hazards and the risk of health effects on the riverine population were consistently higher in the Ulindi river basin (gold mining), in comparison to the Dilala and the Luilu river basins (cobalt and copper mining) [10].

Based on the ambient radiation dose rate (ODRA), the annual exposure of population members averaged 8.4 (range 0.5–40) mSv y^{-1}, well above the world average dose rate of 2.4 mSv y^{-1} [30]. The workers involved in artisanal gold mining at the Ulindi River receive doses at the upper end of the dose range, while members of the population are likely to be less exposed and might receive doses towards the lower end of the dose range.

The current study did not include indoor radon measurements. However, the hazard index H_{in} values indicated that river sediment residues from Ulindi River and some soils are not as suitable as construction materials (Table 4). Their use in house building will increase human exposure through inhalation of indoor radon (^{222}Rn and ^{220}Rn), which may even duplicate the dose received from the ambient radiation, ODRA (See, for example, Van Dung [50]).

This external exposure to ionizing radiation by the Ulindi river is comparable to dose rates of regions designated as high natural radiation background areas (HBRA) [51]. There are several HBRA regions well identified and investigated, either to characterize radiation exposure or to search health effects in the population from prolonged exposure to radiation. Among these areas, one counts Ramsar in Iran, Guarapari in Brazil, Auvergne in France, Xinjiang in China, and Bat Xat in Vietnam [50]. Radiation dose rates reported from these areas range approximately from 5 mSv y^{-1} to about 250 mSv y^{-1}, but biological effects in humans have been hard to identify in a conclusive manner, in general because

either accurate morbidity statistics are missing or the exposed population is of a reduced number [52].

Titanium was present in high concentrations in soils (470 ± 118 mg kg^{-1}) and in sediments (275 ± 104 mg kg^{-1}) (Table 5). U and Th were associated with titanium, particularly in sediments, and this association was statistically significant ($p < 0.05$). The fixation of U by Ti in the sediment cycle has been reported for several sedimentary regimes, and it is known to be very stable [53,54]. This association occurs during the erosion of granites and is stable even under extreme chemical and physical conditions, allowing for the joint transportation of U and Ti from the granite and schist deposits, followed by eventual mineralization in quartz's veins, and later transport with sediments and accumulation in alluvial deposits. Th also seems to follow the geochemical pathways of Ti.

Table 5. Ti, U, and Th mass concentrations (mg kg^{-1} dry weight) in soil and sediment samples. Ti and Th mass concentrations were determined by ICP-MS, and U mass concentration was calculated using gamma spectrometry results.

Sampling Site	Sample Label	Titanium	Uranium (*)	Thorium
Camp Ngano 1	So1	538.39	3.04	19.6
Camp Ngano 2	So2	192.56	-	-
River Andamane	So3	472.42	1.70	25.9
Kamundala Beach	So4	478.31	2.37	10.3
Chantier Malu	So5	521.98	4.15	29.4
Makoma 1	So6	509.35	4.62	67.2
Makoma 2	So7	575.82	5.14	28.4
Camp Ngano 1	Se1	248.97	14.85	339.2
Camp Ngano 2	Se2	406.31	59.25	-
River Andamane	Se3	111.29	2.92	105.4
Kamundala Beach	Se4	195.75	5.17	115.3
Chantier Malu	Se5	340.41	57.24	494.0
Makoma 1	Se6	404.27	123.52	526.3
Makoma 2	Se7	219.40	8.89	152.1
All soils	Average	470	3.5	30.1
	Minimum	192.56	1.70	10.3
	Maximum	575.82	5.14	67.2
All sediments	Average	275	39	288.7
	Minimum	111.29	2.92	105.4
	Maximum	406.31	123.52	526.3

(*) Calculated based on the activity concentrations (Bq kg^{-1}) of ^{238}U in samples, considering that ^{238}U contributes to 0.99275 to the mass of natural uranium and that the specific activity of natural uranium is 25.5 kBq g^{-1}.

The presence of high concentrations of U in riverbed sediments and its manipulation during gold mining, and especially the use of river water as drinking water, may allow for the accumulation of U and co-occurring metals in the human body. There are no data for the population from the eastern Congo, and information on accumulation of these metals in humans in general is scarce for the country. The first biomonitoring in the copper belt region was focused on the miner's population of Kolwezi town, compared with a reference population living far from the copper mining area. Levels of Co, Cu, Cd, Pb, As, and U were enhanced in the urine of miners, including children, and the Co levels were even the world highest in a general population [8]. The higher levels of uranium in body fluids were reported for people living closer to copper mines and statistically significant correlations were found between levels of uranium in urine and in drinking water [8,12].

3.3. Statistical Correlation

In order to determine the relationships and strength of association between paired variables, the Spearman rank-order correlation was calculated. The results are shown in Table 6.

A positive correlation, significant at $p < 0.05$, was observed between ^{238}U and ^{226}Ra, which is not surprising because both radionuclides are members of the same radioactive decay series (uranium series), and thus originate from the same geological sources.

Table 6. Spearman rank-order correlation coefficients between radiological variables in soil and sediments samples.

Variables	^{226}Ra	^{232}Th	^{40}K	Ra_{Eq}	ODRA	AEDE	ELCR	H_{ex}	H_{in}
^{238}U	**0.900**	**0.544**	0.038	**0.901**	**0.911**	**0.895**	**0.906**	**0.911**	**0.890**
^{226}Ra		**0.451**	−0.072	**0.872**	**0.871**	**0.834**	**0.859**	**0.871**	**0.949**
^{232}Th			−0.440	**0.747**	**0.746**	**0.742**	**0.749**	**0.746**	**0.654**
^{40}K				−0.198	−0.201	−0.177	−0.198	−0.201	−0.198

Statistically significant coefficients ($p < 0.05$) are in bold.

The positive correlation ($p < 0.05$) between ^{238}U and ^{232}Th and between ^{232}Th and ^{226}Ra can be explained by the fact that these radionuclides originate in the same geological sources and, furthermore, they are likely transferred through the same pathways in the environment. As discussed above, both U and Th were positively correlated with Ti concentrations in the riverbed sediment.

Radioactive ^{40}K displays no significant correlation with radiological parameters, while positive correlations ($p < 0.05$) were observed between ^{238}U, ^{232}Th, and ^{226}Ra activity concentrations with all radiological indices (Ra_{Eq}, ODRA, AEDE, ELCR, H_{ex}, and H_{in}). These correlations follow the very strong contribution from these three radionuclides to the radiological parameter indices. Indeed, from the data it is clear that these three radionuclides are the main contributors to the gamma dose at all sampling sites.

4. Conclusions

The activity concentrations and environmental distribution of key natural radionuclides (^{238}U, ^{226}Ra, ^{210}Pb, ^{232}Th, and ^{40}K) were determined using gamma-ray spectrometry and inductively coupled plasma–mass spectrometry in the analysis of soil and sediment samples from the Ulindi river basin, at the Maniema and South Kivu provinces in eastern Democratic Republic of the Congo.

The concentrations of the three primordial radionuclides ^{238}U, ^{232}Th, and ^{40}K were far above the worldwide average concentrations in soils compiled by UNSCEAR. Furthermore, the highest concentration values of almost all radionuclides were measured at locations where artisanal and small-scale gold mining activities were carried out, confirming the co-occurrence of radionuclides (U, Th, and their progeny) with non-radioactive metals, such as Ti, in the gold placers targeted by mining activities. The co-occurrence of primordial radioactive elements with stable metals is not uncommon and has been reported from other regions.

The radiological parameters Ra_{Eq}, ODRA, AEDE, ELCR, H_{ex}, and H_{in} were calculated to evaluate the radiological hazards from exposure to radioactivity in sediments and soils to the mining workers and to members of the local population. The average and the range of all radiological parameters showed much higher values than the world average level (used as a reference level) for each parameter. Based on radioactivity levels and ambient dose rate levels, the upper reach of Ulindi River basin may be classified as a region with a natural high radiation background.

Clayey soils and sediments from the areas investigated in the Ulindi River are not suitable for use as construction materials. However, the area investigated in the Andamane River basin is not of high radiation background and geological materials from there are suitable for use as construction materials.

These results clearly show that the artisanal and small-scale gold mining activities in this region, although targeting a non-radioactive metal, originate enhanced radiation exposures of miners and their co-workers exceeding the radiation safety standards. Fur-

thermore, the use of river sediments to build houses increases the radiological hazards to riverine populations. Therefore, a radiation safety policy and a regional implementation strategy seem needed to avert the exposure of local population to ionizing radiations above the internationally agreed safety standards.

Author Contributions: Conceptualization: E.K.A., F.P.C., J.P., P.T.M. and C.K.M.; sampling: E.K.A.; sample preparation, formal analysis, and data validation: E.K.A., J.-L.L., J.P. and P.A.; methodology and data interpretation: E.K.A., J.-L.L., J.P. and F.P.C.; writing—original draft: E.K.A.; writing—review and editing: E.K.A., F.P.C. and J.-L.L. All authors have read and agreed to the published version of the manuscript.

Funding: This research received no external funding.

Data Availability Statement: Not applicable.

Acknowledgments: The analytical work was performed in the analytical platform of University of Geneva, Switzerland.

Conflicts of Interest: The authors declare no conflict of interest.

References

1. Milesi, J.P.; Toteu, S.F.; Deschamps, Y.; Lerouge, C.F.; Cocherie, A.; Penaye, J.; Tchameni, R.; Moloto-A-Kenguemba, G.; Kampunzu, H.A.B.; Nicol, N. An overview of the geology and major ore deposits of Central Africa: Explanatory note for the 1:4,000,000 map "Geology and major ore deposits of Central Africa. *J. Afr. Earth Sci.* **2006**, *44*, 571–595. [CrossRef]
2. Yager, T.R. The Mineral Industry of Congo (Kinshasa). United States Geological Survey Minerals Yearbook—2017–2018. USA Government. 2022. Available online: https://pubs.usgs.gov/myb/vol3/2017-18/myb3-2017-18-congo-kinshasa.pdf (accessed on 22 August 2022).
3. *World Mining Data*; Federal Ministry of Agriculture, Regions and Tourism: Vienna, Austria, 2020.
4. IPIS. Analysis of the Interactive Map of Artisanal Mining Areas in Eastern DR Congo. 2015 Update. International Peace Information Service (IPIS): Antwerp, The Netherlands, 2016. Available online: https://ipisresearch.be/wp-content/uploads/2016/10/Mapping-minerals-in-eastern-DR-Congo_v005.pdf (accessed on 22 August 2022).
5. Global Witness. River of Gold. London, UK. 2016. Available online: https://www.globalwitness.org/en/campaigns/conflict-minerals/river-of-gold-drc/ (accessed on 22 August 2022).
6. Karaki, K. Artisanal Gold Mining in DRC: Time to Get Down to Earth. *European Centre for Development Policy Management (ECDPM)*. Discussion Paper No. 223. 2018. Available online: https://ecdpm.org/wp-content/uploads/DP-223-Artisanal-gold-mining-in-DRC.pdf (accessed on 22 August 2022).
7. Meneghel, L. Proterozoic strata-bound uranium deposits of Zambia and Zaire. In *Proterozoic Unconformity and Stratabound Uranium Deposits. IAEA-Tecdoc-315*; International Atomic Energy Agency: Vienna, Austria, 1984; pp. 7–34.
8. Banza, C.L.N.; Nawrot, T.S.; Haufroid, V.; Sophie, D.; De Putter, T.; Smolders, E.; Kabyla, B.I.; Luboya, O.N.; Ilunga, A.N.; Mutombo, A.M.; et al. High human exposure to cobalt and other metals in Katanga, a mining area of the Democratic Republic of Congo. *Environ. Res.* **2009**, *109*, 745–752. [CrossRef] [PubMed]
9. Tsurukawa, N.; Prakash, S.; Manhart, A. *Social Impacts of Artisanal Cobalt Mining in Katanga, Democratic Republic of the Congo*; Oko-Institut e.V./Institute for Applied Ecology: Freiburg, Germany, 2011.
10. Atibu, E.K.; Oliveira, J.M.; Malta, M.; Santos, M.; Mulaji, C.K.; Mpiana, P.T.; Carvalho, F.P. Assessment of natural radioactivity in the copper belt region, Kolwezi Province, of the Democratic Republic of the Congo. *J. Geosci. Environ. Prot.* **2021**, *9*, 1–20. [CrossRef]
11. UNEP. *Assessment Mission of the Shinkolobew Uranium Mine. Democratic Republic of the Congo, November 2004*; UNEEP/OCHA Environment Unit: Geneva, Switzerland, 2004.
12. Banza, L.N.C.; Casas, L.; Haufroid, V.; De Putter, T.; Saenen, N.D. Sustainability of artisanal mining of cobalt in DR Congo. *Nat. Sustain.* **2018**, *1*, 495–504. Available online: http://hdl.handle.net/2078.1/213422 (accessed on 22 August 2022). [CrossRef] [PubMed]
13. CosocGl (Coalition de la Société civile de la Région des Grands lacs Contre L'exploitation illégales des Ressources Naturelles). La ruée vers l'Or à Shabunda, Pratiques et impacts de L'exploitation Minière par Dragues. 2015. Available online: http://afrikarabia.com/wordpress/wp-content/uploads/2015/10/Etude_draguesShabunda.pdf (accessed on 11 March 2020).
14. USFDA. *Biological Effects of Ionizing Radiation; United States Food and Drug Administration*; HEW Publication (FDA): Silver Spring, MD, USA, 2006; pp. 77–8004.
15. IAEA. *Radiation Protection and Safety of Radiation Sources: International Basic Safety Standards*; IAEA Safety Standards Series No. GSR Part 3; International Atomic Energy Agency: Vienna, Austria, 2014.

16. Tshonda, J.O.; Buleli, L.N.; Kalombo, V.; Akilimali, C.; Kyaga, K.; Omaka, T.; M'pene, Z.; Krawczyk, J.; Laghmouch, M. Maniema, Espaces et vies. Le Cri Édition. 2011. Léopold Wiener 18 Avenue, Brussels B-1170, Belgium. Available online: https://www.africamuseum.be/sites/default/files/media/docs/research/publications/rmca/online/monographies-provinces/maniema.pdf (accessed on 11 March 2020).
17. Villeneuve, M.; Wazi, N.; Kalikone, C.; Gärtner, A. A Review of the G4 "Tin Granites" and Associated Mineral Occurrences in the Kivu Belt (Eastern Democratic Republic of the Congo) and Their Relationships with the Last Kibaran Tectono-Thermal Events. *Minerals* **2022**, *12*, 737. [CrossRef]
18. Nkuba, B.; Bervoets, L.; Sara Geenen, S. Invisible and ignored? Local perspectives on mercury in Congolese gold mining. *J. Clean. Prod.* **2019**, *221*, 795–804. [CrossRef]
19. Jansson, J.; Burke, C.; Jiang, W. *Chinese Companies in the Extractive Industries of Gabon & the DRC: Perceptions of Transparency*; Centre for Chinese Studies, University of Stellenbosch: Stellenbosch, South Africa, 2009; p. 55.
20. Atibu, E.K.; Devarajan, N.; Laffite, A.; Giuliani, G.; Salumu, J.A.; Muteb, R.C.; Mulaji, C.K.; Otamonga, J.-P.; Elongo, V.; Mpiana, P.T.; et al. Assessment of trace metal and rare earth elements contamination in rivers around abandoned and active mine areas. The case of Lubumbashi River and Tshamilemba Canal, Katanga, Democratic Republic of the Congo. *Chem. Erde* **2016**, *76*, 353–362. [CrossRef]
21. Atibu, E.K.; Gregory, G.; Mulaji, C.K.; Otamonga, J.P.; Elonga, V.; Mpiana, P.T.; Poté, J. Impact assessment of an area contaminated by abandoned mine: Case of the Dilala, Mpingiri and Luilu rivers, district of Kolwezi, Democratic Republic of the Congo. *Chemosphere* **2018**, *191*, 1008–1020. [CrossRef]
22. Carvalho, F.P. 210Pb and 210Po in sediments and suspended matter in the Tagus estuary, Portugal. Local enhancement of natural levels by wastes from phosphate ore processing industry. *Sci. Total Environ.* **1995**, *159*, 201–214. [CrossRef]
23. Sima, O.; Arnold, D.; Dovlete, C. GESPECOR: A versatile tool in gamma-ray spectrometry. *J. Radioanal. Nucl. Chem.* **2001**, *248*, 359–364. [CrossRef]
24. Adler, A.; Devarajan, N.; Wildi, W.; Poté, J. Metal Distribution and Characterization of Cultivable Lead-Resistant Bacteria in Shooting Range Soils. *Soil Sediment Contam. Int. J.* **2016**, *25*, 378–394. [CrossRef]
25. Poté, J.; Haller, L.; Loizeau, J.-L.; Bravo, A.G.; Sastre, V.; Wildi, W. Effects of a sewage treatment plant outlet pipe extension on the distribution of contaminants in the sediments of the Bay of Vidy, Lake Geneva, Switzerland. *Bioresour. Technol.* **2008**, *99*, 7122–7131. [CrossRef] [PubMed]
26. Belyaeva, O.; Pyuskyulyan, K.; Movsisyan, N.; Saghatelyan, A.; Carvalho, F.P. Natural radioactivity in urban soils of mining centers in Armenia: Dose rate and risk assessment. *Chemosphere* **2019**, *225*, 859–870. [CrossRef] [PubMed]
27. Taqi, A.H.; Shaker, A.M.; Battawy, A.A. Natural radioactivity assessment in soil samples from Kirkuk city of Iraq using HPGe detector. *Int. J. Radiat. Res.* **2018**, *16*, 4.
28. UNSCEAR. Sources and effects of ionizing radiation. In *United Nations Scientific Committee on the Effects of Atomic Radiation, Report to the General Assembly with Annexes*; United Nations: New York, NY, USA, 2000.
29. Issa, S.; Uosif, M.; Elsaman, R. Gamma radioactivity measurements in Nile River sediment samples. *Turk. J. Eng. Env. Sci.* **2013**, *37*, 109–122.
30. Ramasamy, V.; Suresh, G.; Meenakshisundaram, V.; Ponnusamy, V. Horizontal and Vertical Characterization of Radionuclides and Minerals in River Sediments. *Appl. Radiat. Isot.* **2011**, *69*, 184–195. [CrossRef]
31. UNSCEAR. Sources and Effects of Ionizing Radiation. In *United Nations Scientific Committee on the Effects of Atomic Radiation Report to the General Assembly with Annexes*; United Nations: New York, NY, USA, 2010.
32. UNSCEAR. Sources and Effects of Ionizing Radiation. In *United Nations Scientific Committee on the Effects of Atomic Radiation, Report to the General Assembly with Annexes*; United Nations: New York, NY, USA, 1993.
33. ICRP. *Recommendations of the International Commission on Radiological Protection*; International Commission on Radiological Protection Publication: Oxford, UK, 1991.
34. Taskin, H.; Karavus, M.; Ay, P.; Topuzoglu, A.; Hidiroglu, S.; Karahan, G. The investigation of radionuclide concentrations in soil and lifetime cancer risk due to gamma radioactivity in Zonguldak, Turkey. *J. Environ. Radioact.* **2009**, *100*, 49–53. [CrossRef]
35. Beretka, J.; Mathew, P.J. Natural Radioactivity of Australian Building Materials, Industrial Wastes and By-Products. *Health Phys.* **1985**, *48*, 87–95. [CrossRef]
36. Sureshghandhi, M.; Ravisanker, R.; Rajalakshmi, A.; Sivakumar, S.; Chandrasekaran, A.; Pream Anand, D. Measurements of natural gamma radiation in beach sediments of north east coast of Tamilnadu, India by gamma ray spectrometry with multivariate statistical approach. *J. Radiat. Appl. Sci.* **2014**, *7*, 7–17. [CrossRef]
37. WHO. *WHO Handbook on Indoor Radon: A Public Health Perspective*; World Health Organization: Geneva, Switzerland, 2019.
38. Agbalagba, E.O.; Onoja, R.A. Evaluation of natural radioactivity in soil, sediment and water samples of Niger Delta (Biseni) flood plain lakes. *Nigeria. J. Environ. Radioact.* **2011**, *102*, 667–671. [CrossRef]
39. Addinsoft: 2020. XLSTAT Statistical and Data Analysis Solution. New York, NY, USA. 2020. Available online: https://www.xlstat.com (accessed on 11 March 2020).
40. Carvalho, F.P. Environmental Radioactive Impact Associated to Uranium Production. *Am. J. Environ. Sci.* **2011**, *7*, 547–553. [CrossRef]
41. Carvalho, F.P. Mining industry and sustainable development: Time for change. *Food Energy Secur.* **2017**, *6*, 61–77. [CrossRef]

42. Carvalho, F.P.; Tufa, M.B.; Oliveira, J.M.; Malta, M. Radionuclides and radiation exposure in tantalite mining, Ethiopia. *Arch. Environ. Contam. Toxicol.* **2021**, *81*, 648–659. [CrossRef] [PubMed]
43. Focus, E.; Rwiza, M.J.; Mohammed, N.K.; Banzi, F.P. The influence of gold mining on radioactivity of mining sites soil in Tanzania. *Int. J. Environ. Qualit.* **2021**, *46*, 46–59. [CrossRef]
44. Lozano, J.C.; Blanco Rodriguez, P.; Vera Tomé, F. Distribution of Long-Lived Radionuclides of the 238 U Series in the Sediments of a Small River in a Uranium Mineralized Region of Spain. *J. Environ. Radioact.* **2002**, *63*, 153–171. [CrossRef]
45. Ademola, A.K.; Bello, A.K.; Adejumobi, A.C. Determination of natural radioactivity and hazard in soil samples in and around gold mining area in Itagunmodi, south-western, Nigeria. *J. Radiat. Res. Appl. Sci.* **2014**, *7*, 249–255. [CrossRef]
46. Kamunda, C.; Mathuthu, M.; Madhuku, M. An Assessment of Radiological Hazards from Gold Mine Tailings in the Province of Gauteng in South Africa. *Int. J. Environ. Res. Public Health* **2016**, *13*, 138. [CrossRef]
47. Faanu, A.; Adukpo, O.K.; Tettey-Larbi, L.; Lawluvi, H.; Kpeglo, D.O.; Darko, E.O.; Emi-Reynolds, G.; Awudu, R.A.; Kansaana, C.; Amoah, P.A.; et al. Natural radioactivity levels in soils, rocks and water at a mining concession of Perseus gold mine and surrounding towns in Central Region of Ghana. *SpringerPlus* **2016**, *5*, 98. [CrossRef]
48. Wanyama, C.K.; Makokha, J.W.; Masinde, F. A radiological survey in tailings: A case study of Rosterman gold mine, western Kenya. *Open Access Libr. J.* **2020**, *7*, 1–9. [CrossRef]
49. Carvalho, F.P.; Oliveira, J.M.; Malta, M. Intake of radionuclides with the diet in uranium mining areas. *Procedia Earth Planet. Sci.* **2014**, *8*, 43–47. [CrossRef]
50. Van Dung, N.; Thuan, D.D.; Nhan, D.D.; Carvalho, F.P.; van Thang, D.; Quang, N.H. Radiation exposure in a region with natural high background radiation originated from rare earth element deposits at Bat Xat district, Vietnam. *Radiat. Environ. Biophys.* **2022**, *61*, 309–324. [CrossRef] [PubMed]
51. Sohrabi, M. World high background natural radiation areas: Need to protect public from radiation exposure. *Radiat. Meas.* **2013**, *50*, 166–171. [CrossRef]
52. Zlobina, A.; Farkhutdinov, I.; Carvalho, F.P.; Wang, N.; Korotchenko, T.; Baranovskaya, N.; Farkhutdinov, A. Impact of Environmental Radiation on the Incidence of Cancer and Birth Defects in Regions with High Natural Radioactivity. *Int. J. Environ. Res. Public Health* **2022**, *19*, 8643. [CrossRef] [PubMed]
53. Ruhlmann, F. Quelques exemples de relation uranium-titanium. *Bull. Minéralogie* **1980**, *103*, 240–244. [CrossRef]
54. Fuchs, S.; Schumann, D.; Williams-Jones, A.E.; Vali, H. The growth and concentration of uranium and titanium minerals in hydrocarbons of the Carbon Leader Reef, Witwatersrand Supergroup, South Africa. *Chem. Geol.* **2015**, *393–394*, 55–66. [CrossRef]